Tuning circular Bragg phenomenon of TiO_2 sculptured thin films with chiral structure

Difan Luo (罗迪帆), Chendi Huang (黄辰迪), and Shaoji Jiang (江绍基)*

State Key Laboratory of Optoelectronic Materials and Technologies,
Sun Yat-sen University, Guangzhou 510275, China
**Corresponding author: stsjsj@mail.sysu.edu.cn*

Received November 11, 2012; accepted December 25, 2012; posted online April 19, 2013

TiO_2 chiral sculptured thin films (CSTFs) prepared using glancing angle deposition (GLAD) method based on electron beam evaporation are studied. The relationship between structural parameters and circular Bragg phenomenon (CBP) is investigated. Results demonstrate that, the central wavelength of Bragg regime red-shifts with the increasing pitch of helix, and peak value of selective transmittance will increase after adding more turns to the helix. After annealing, the central wavelength blue-shifts and the peak value rises. Tuning CBP by modulating the deposition parameters and annealing can optimize the performance of circularly polarized devices fabricated from CSTFs.

OCIS codes: 310.1860, 310.5448, 160.1585.
doi: 10.3788/COL201311.S10102.

Glancing angle deposition (GLAD) is a simple but powerful technology, which is based on physical vapor deposition, to prepare micro-nano structure thin films. By combining the oblique angle deposition and the substrate rotation, sculptured thin film (STF) with anisotropy structure can be formed[1,2]. It was first reported in 1959 by Young *et al.*, who experimentally verified its feasibility[3]. At the end of the 20th century, the research of STF was developed rapidly. The researchers demonstrated that due to the atomic shadowing effect and low surface atomic mobility, STF was characterized as high porosity, large surface area, and anisotropic properties, which could be widely applied in optical, biological, and energy fields[4−7].

Hodgkinson *et al.* were the first to employ the substrate rotation based on the large oblique angle and deposited chiral sculptured thin films (CSTFs), also known as helical thin films[8]. They found that the films exhibited circular Bragg phenomenon (CBP) and tended to have transmission responses which were selectively polarizing in Bragg regime. With the ability to discriminate different circularly polarization states, CSTFs are suitable for the preparation of circular polarizer, including filters, reflectors, and sensors[9−11].

In this letter, a series of TiO_2 CSTFs is fabricated using GLAD technique. Mechanically, we analyze the different chiral structures by varying the experimental parameters, and study the effect of the pitch, turns, and annealing upon CBP of films.

Two independent stepper motors were built in the vacuum chamber of an electron beam evaporation system (ZZSX-700), ensuring accurate control of deposition angle and substrate rotation, respectively. TiO_2 was chosen as the source material, because of its high refractive index and low absorption in the visible and near-infrared region. In the process of this experiment, electron beam evaporation resulted in decomposition, which further causing oxygen-deficiency of TiO_2 and forming Ti_4O_7 with high absorption[12]. Amount of oxygen was used as experiment atmosphere and the vacuum pressure was kept relatively low at 1.0×10^{-2} Pa. To ensure the shadowing effect, the deposition angle is maintained at 80° from the normal surface of the substrate. And cleaned glasses and polished Si wafers were employed as substrate. The substrate rotated in low speed of 0.07 rpm clockwise, such that the helix was right handed. To isolate the helix by low surface atomic mobility, TiO_2 CSTFs was deposited at room temperature.

Table 1 lists six TiO_2 samples prepared by GLAD technique with various deposition parameters. In samples 1–3, the deposition rate was set to increase gradually, in order to form a set of films with the same turns and variable pitch. In samples 2 and 4–6, the deposition rate remained the same while the thickness varied, to form a set of films with the decreasing turns from 6 to 3. To analyze the annealing effect on the magnitudes of CBP, the samples were annealed for 4 h at a temperature of 280 °C after initial fabrication.

The morphology and structure of the samples were characterized using scanning electron microscope (SEM, Quanta 400F) and profilometer (XP-200). Spectra measurements were observed by a spectrophotometer (Lambda 900 UV/VIS/NIR), which can generate left circular polarization (LCP) and right circular polarization (RCP) light by placing a Glan-Taylor prism and a quarter-wave plate in beam path.

SEM images of sample 1 are shown in Fig. 1,

Table 1. TiO_2 CSTFs Samples with Deposition Parameters

Sample	Number of Turns	Pitch (nm)	Thickness (μm)	Deposition Rate (nm/s)
1	6	265	1.59	0.31
2	6	280	1.68	0.32
3	6	292	1.75	0.34
4	5	280	1.40	0.32
5	4	280	1.12	0.32
6	3	280	0.84	0.32

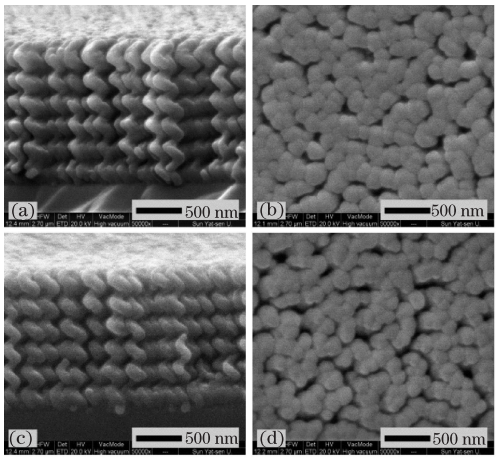

Fig. 1. Side-view (left column) and top-view (right column) SEM images of sample 1. (a) and (b): pre-annealing; (c) and (d): post-annealing.

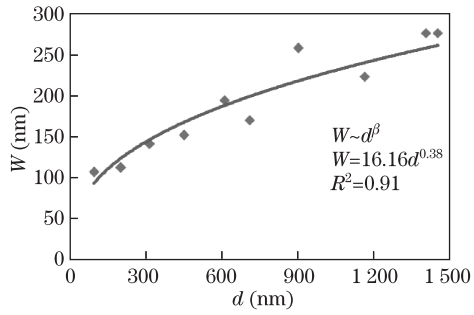

Fig. 2. Average helical column width W as a function of column length d for the TiO_2 CSTF.

demonstrating that TiO_2 CSTFs consist of arrays of helical nanorods that parallel and nominally identical to each other, due to the shadowing effect and competitive growth mechanism. Compared with the pre-annealing samples, the morphology of post-annealing samples in Figs. 1(c) and (d) behave thinner columns and higher porosity with the same thickness.

The size of helical column diameter is an important parameter of CSTF, along with the continuous growth of the film in the vertical direction, the helical nanorods gradually broadening, and the relationship following a power scaling law[13]:

$$W \propto d^{\beta}, \tag{1}$$

where W is column width, d is column length, and β denotes growth exponent, relating to material itself. For the side-view image in Fig. 1(a) of sample 1, the average of 5–8 columns width were measured in 10 different heights. Figure 2 depicts the exponential relationship between the column width and length. Regression curve resulted in a β of 0.38, in line with the growth exponent of TiO_2 vertical thin film in the same deposition angle[14].

The reason that helical columns broaden laterally through the thickness increases is as follow: as the film grows, the increase of scattering results in the rise of substrate temperature, so does the surface atomic mobility, which leads to broadening in the helical column. In addition, the competitive growth mechanism may also contribute to this morphology while it generally occurs in the film with more turns than ours.

TiO_2 STFs with chiral structure exhibited different behaviors with LCP and RCP incident light, the representative selective transmittance spectrum is displayed in Fig. 3, where the vertical axis is the different percentages of LCP versus RCP transmittance. These right handed CSTFs transmit LCP light while reflecting RCP light in Bragg regime, and the central wavelength red-shifts as the pitch of helix increase (sample 1–3), from 430 to 480 nm. The dependence of the central wavelength λ^{Br}, on the pitch of helix P[15] is shown as

$$\lambda^{Br} = n_{eff} \cdot P, \tag{2}$$

where n_{eff} is the effective refractive index of the film, thus the result of these samples is 1.6, which is lower than that of TiO_2 bulk material because of the large porosity in film. Furthermore, the peak value of selective transmittance is not affected by varying pitch, keeping at about 12.5%.

The rise of the number of turns to the CSTFs will enhance the response of CBP. As revealed in Fig. 4, with the increase of the turns, the central wavelength remains at 461 nm, while the peak value of selective transmittance behaves stronger obviously. From 3 turns (sample 6) to 6 turns (sample 2), the peak value ascends by approximately twice, from 4.8% to 12.5%. And the magnitude of CBP of sample 2 is higher than others. So, altering the numbers of turns will affect the peak value of selective transmittance instead of the central wavelength. It suggests that these STFs with controllable chiral structure can be fabricated to tune CBP.

After thermal annealing, the chiral structure of TiO_2 STFs changed, affecting CBP. The researchers found that annealing at high temperature would change the TiO_2

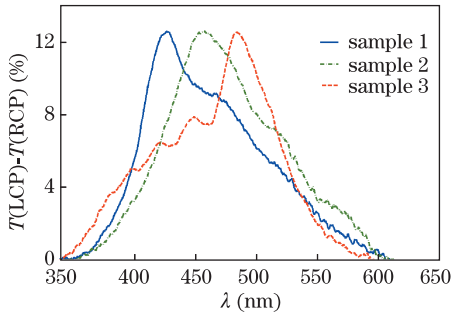

Fig. 3. (Color online) Selective transmittance spectra of TiO_2 CSTFs with different pitchs of helix (sample 1–3).

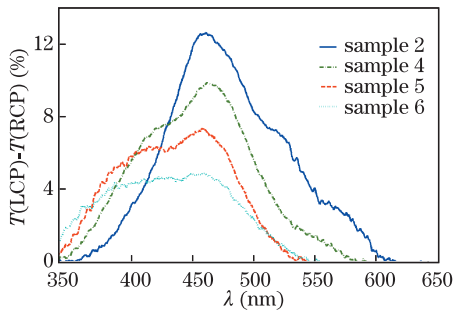

Fig. 4. (Color online) Selective transmittance spectra of TiO_2 CSTF with different turns of helix (sample 2, 4, 5, and 6).

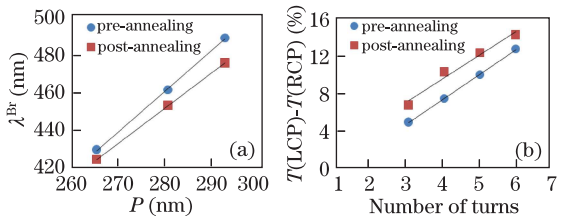

Fig. 5. (a) Central wavelength as a function of pitch of sample $1-3$; (b) peak values of selective transmittance as a function of turns of sample 2, 4, 5, and 6.

thin film from amorphous to crystalline with anatase phase[16]. To avoid this change, the annealing temperature was set as 280 °C. Figure 5(a) presents the pre- and post-annealing relationship between the central wavelength and the pitch, with a lower λ^{Br} of CBP after annealing. Figure 5(b) illustrates that the peak values of selective transmittance plotted as a function of the number of turns before and after annealing. The trend suggests that compared with the pre-annealing samples, the maximum T(LCP)-T(RCP)% of TiO_2 CSTFs had been significantly raised after annealing.

The effect of annealing on CBP can be analyzed from the mechanism of thin film growth that annealing changed the nanostructure of CSTFs. As shown in Fig. 1 and discussed above, the porosity of films increased and the size of column diameter decreased after annealing. Consequently, the λ^{Br} of Bragg regime blue-shifted with columnar thinning[17]. In addition, thermal anneal treatment can eliminate the suboxide in TiO_2 and reduce the absorption of film, yielding the increase of the maximum T(LCP)-T(RCP)%.

In conclusion, a series of TiO_2 STFs with chiral structures is fabricated by GLAD technique. The coarsening phenomenon in films caused by scattering is investigated. By measuring the response of different circular polarized incident lights for the CSTFs, the relationships between the structural parameters and CBP are studied. Results show that, right handed CSTFs exhibit strong CBP in Bragg regime while reflecting RCP light and transmitting LCP light. The central wavelength is linear with the pitch of helix, and it red-shifts as the increase of pitch. More number of turns in the helix enhances the strength of CBP with the ascent of the peak value of selective transmittance, from 4.8% to 12.5%. Besides, the helical columns become thinner and the absorption of CSTFs drops after annealing, leading to the blue-shift of the central wavelength and the increase of the peak value of selective transmittance. Modification of the deposition parameters and annealing is used to control the pitch and the turns of the helix, which can tune CBP for the optimization of the circularly polarized device made by CSTFs.

This work was supported by the National Natural Science Foundation of China under Grant Nos. 61275159, 60977042, and 11074311.

References

1. M. M. Hawkeye and M. J. Brett, J. Vac. Sci. Technol. A **25,** 1317 (2007).
2. J. J. Steele and M. J. Brett, J. Mater. Sci. Mater. Electron. **18,** 367 (2007).
3. N. O. Young and J. Kowal, Nature **183,** 104 (1959).
4. K. Robbie, M. J. Brett, and A. Lakhtakia, Nature **384,** 616 (1996).
5. D. P. Smetaniuk, M. T. Taschuk, and M. J. Brett, IEEE Sen. J. **11,** 1713 (2011).
6. W. Zhang, S. Kim, N. Ganesh, I. D. Block, P. C. Mathias, H.-Y. Wu, and B. T. Cunningham, J. Vac. Sci. Technol. A **28,** 996 (2010).
7. L. González-García, I. González-Valls, M. Lira-Cantu, A. Barranco, and A. R. González-Elipe, Energy Environ. Sci. **4,** 3426 (2011).
8. I. Hodgkinson, Q. H. Wu, B. Knight, A. Lakhtakia, and K. Robbie, Appl. Opt. **39,** 642 (2000).
9. L. O. Palomares and J. A. Reyes, Appl. Phys. Lett. **93,** 181909 (2008).
10. Y. J. Park, K. M. A. Sobahan, and C. K. Hwangbo, Opt. Express **16,** 5186 (2008).
11. A. Lakhtakia, M. W. McCall, J. A. Sherwin, Q. H. Wu, and I. J. Hodgkinson, Opt. Commun. **194,** 33 (2001).
12. J. Tang, P. Gu, X. Liu, and H. Li, *Modern Optical Thin Film Technology* (in Chinese) (Zhejiang University Press, Hangzhou, 2006).
13. T. Karabacak, J. P. Singh, Y.-P. Zhao, G.-C. Wang, and T.-M. Lu, Phys. Rev. B **68,** 125408 (2003).
14. M. T. Taschuk, K. M. Krause, J. J. Steele, and M. A. Summers, J. Vac. Sci. Technol. B **27,** 2106(2009).
15. A. C. van Popta, M. J. Brett, and J. C. Sit, J. Appl. Phys. **98,** 083517 (2005).
16. M. Suzuki, T. Ito, and Y. Taga, J. J. Appl. Phys. Pt. 2 **40,** L398 (2001).
17. A. Lakhtakia and M. W. Horn, Optik **114,** 556 (2003).